中 國 醫 藥 大 學

專題研究計畫成果報告

計畫名稱：以調控缺氧誘發因子(HIF-1α)的觀點探討低能雷射治療慢性發炎及疼痛的分生機制

已經發表於

Hsieh YL, Chou LW, Chang PL, Yang CC, Kao MJ, Hong CZ. Low-level laser therapy alleviates neuropathic pain and promotes function recovery in rats with chronic constriction injury-possible involvements in hypoxia-inducible factor 1α (HIF-1α). J Comp Neurol. 2012 Feb 20. doi: 10.1002/cne.23072. [Epub ahead of print]

計畫編號：CMU99-TC-23

執行期限：100 年 04 月 01 日至 101 年 03 月 31 日

單位名稱：物理治療學系

主持人：謝悅齡

中　華　民　國 101 年 04 月 14 日

Abstract

Background. Nerve inflammation plays an important role in the development and progression of neuropathic pain after chronic constrictive injury (CCI). Recent studies explored hypoxia-inducible factor 1α (HIF-1α) in the process of inflammation. Low-level laser therapy (LLLT) has been suggested to benefit treatment of pain disorders, but few data directly support LLLT for neuropathic pain. ***Objective.*** We investigated the effect of LLLT on accumulation of hypoxia-inducible factor-1 alpha (HIF-1α), proinflammatory cytokines tumor necrosis factor-α (TNF-α), and interleukin-1β (IL-1β) for controlling neuropathic pain, as well as on activation of vascular endothelial growth factor (VEGF) and nerve growth factor for promoting functional recovery in rat model of CCI. ***Methods.*** CCI was induced by placing four loose ligatures around the sciatic nerve of rats. LLLT (660 nm, 9 J/cm^2) at CCI sites was performed after 7 days of CCI. Effects of LLLT in CCI animals were determined by measuring mechanical paw withdrawal threshold (MPWT), sciatic, tibial and peroneal function indexes (SFI, TFI and PFI), and histopathological and immunoassay analyses. ***Results.*** Our results demonstrated that LLLT significantly improved MPWT, SFI, TFI and PFI after CCI. LLLT also significantly reduced overexpressions of HIF-1α, TNF-α and IL-1β and increased the amounts of VEGF, NGF and Schwann cells. ***Conclusions.*** LLLT can modulate HIF-1α activity and may represent a novel, clinically applicable therapeutic approach for improvement of tissue hypoxia/ischemia and inflammation in nerve entrapment neuropathy as well as for promotion of nerve regeneration, which may lead to sufficient morphologic and functional recovery of the peripheral nerve.

Key Words: Chronic constrictive injury —Low-level laser therapy —Hypoxia-inducible factor 1α —Neuropathic pain —Functional recovery

Introduction

Neuropathic pain is a common sequela initiated by a primary lesion of the peripheral or central nervous system (Baron, 2000, Zimmermann, 2001). In previous studies, the relationship between proinflammatory cytokines, such as tumor necrosis factor-α (TNF-α), interleukin 1 (IL-1) released by inflammatory cells on their activation and the development of hyperalgesia and allodynia in neuropathic pain has been identified (Sommer and Kress, 2004, Sommer and Schäfers, 2004, Li et al., 2011, Liou et al., 2011). These results support the notion that nerve inflammation plays an important contributory role in the development and progression of neuropathic pain. Experimentally, various animal models of peripheral neuropathy have been developed. Chronic constriction injury (CCI) of the sciatic nerve with loose ligatures is the most widely used model for peripheral neuropathy and neuropathic pain (Bennett and Xie, 1988, Kingery et al., 1993), simulating the clinical condition of chronic nerve compression as occurs in nerve entrapment neuropathy or spinal root irritation by a lumbar disk herniation (Zimmermann, 2001).

Hypoxia-inducible factor-1α (HIF-1α) is a transcription factor that is increased in conditions of hypoxia, ischemia and inflammation (Fraisl et al., 2009). HIF-1α is also thought to be essential in maintaining inflammatory processes by promoting the production of proinflammatory cytokines, including TNF-α and IL-1β (Takeda et al., 2009). HIF-1α has been identified as a pivotal transcription factor linking the inflammatory pathways (Dehne and Brune, 2009). Inhibition and/or down-regulation of these molecules may exert anti-hypoxic and anti-inflammatory effects. Therefore, inhibiting HIF-1α accumulation may be a novel therapeutic strategy for neuropathic inflammation.

Many experimental and clinical studies have also reported positive effects of low-level laser therapy (LLLT) for promoting the repair processes of peripheral nerve by increasing vascular endothelial growth factor (VEGF) and nerve growth factor (NGF) secretions (Byrnes et al., 2005, Gigo-Benato et al., 2005, Hou et al., 2008, Rochkind, 2009, Rochkind et al., 2009, Gigo-Benato et al., 2010), and by inhibiting the inflammation through reduction of pro-inflammatory cytokines (Albertini et al., 2007). However, to date, there is little evidence directly supporting the anti-allodynia effects of LLLT in neuropathic pain. In this study, therefore, the effects of LLLT on management of neuropathic pain after CCI in sciatic nerve of rat were investigated and possible biological mechanisms through which LLLT may exert its action on functional recovery of peripheral nerve were analyzed. We hypothesized that LLLT can decrease pro-inflammatory cytokines, reduce HIF-1α accumulation, and then promote expressions of VEGF and NGF in the sciatic nerve proximal to the site of CCI on improvement of neuropathic pain and functional recovery.

MATERIALS AND METHODS

General Design

Neuropathy was induced in all animals by CCI surgery. After surgery, animals (n=40) were divided randomly into four groups (Figure 1) based on the nerve surgery and treatment administration: (1) the CL group (n=10), which consisted of CCI animals that received LLLT; (2) CsL group (n=10), which consisted of CCI animals that received sham-irradiated LLLT; (3) sCL group (n=10), which consisted of sham-operated CCI animals that received LLLT; and (4) sCsL group (n=10), which consisted of sham-operated CCI animals that received sham-irradiated LLLT. Treatments of LLLT or sham-irradiation were given for consecutive 7 days. The evaluation instruments were mechanical paw withdrawal threshold (MPWT), sciatic functional index (SFI), tibial functional index (TFI), peroneal functional index (PFI), histology,

immunohistochemistry and immunoassays. Pain and functional assessments were performed the day before (pre-op, at day 0), immediately after operation (post-op, at day 1), at 7 days (7d post-op, at day 7) after surgery and after the 7-day treatment (post-tr, at day 14). Animals were sacrificed for assessments of histopathology and immunoassays the day after completing the treatments. A flow diagram of the experimental design is presented in Figure 1.

Animals

Experiments were performed on adult male Sprague–Dawley rats (SD, 250 to 300 g, purchased from BioLASCO Co., Ltd, Taiwan). Ambient temperature was maintained at 22 to 24 °C and the animals were kept on an artificial 12-h light–dark cycle in the Animal Center of China Medical University. The light period began at 7:00 a.m. with food and water available ad libitum up to the time of testing. Efforts were made to minimize discomfort and reduce the number of animals used. The ethical guidelines of the International Association for Study of Pain in Animals were followed (Zimmermann, 1983). All experimental procedures were approved by the China Medical University Committee on Animal Care and Use.

Chronic Constriction Injury of Sciatic Nerve

Following the procedure originally proposed by Bennet and Xie (Bennett and Xie, 1988) adapted for mice, CCI of sciatic nerve was used as the model of peripheral nerve injury for evoking neuropathic pain symptoms. Surgery was performed under anesthesia with 4% isoflurane in liquid form for inhalation (AErrane, Baxter Healthcare of Puerto Rico, PR). Using a double-headed operating microscope, the sciatic nerve on one randomly selected side was exposed by skin incision along the femur and separation of biceps femoris and superficial gluteal muscles. At the middle third of the sciatic nerve, four ligatures with 4-0 chromic gut thread (Ethicon, USA) were tied loosely around the nerve with inter-ligation spacing of about 1 mm. The wound of muscle layers (with 4/0 reabsorbable suture, Ethicon, USA) and skin (with 3/0 non-reabsorbable suture, Ethicon, USA) were then sutured and closed to allow recovery. Sham-operated CCI animals underwent the same procedures. Branches were dissociated and without any lesion for comparison
.

Low-Level Laser Irradiation

Seven days after surgery, a continuous 660-nm Ga-Al-As diode laser (Aculas-Am series, Multi-channel LLLT system; Konftec Corporation, Taipei, Taiwan) was used in this study. After sterilization, the hand-held delivery probe was placed lightly on the skin surface directly above the loose ligation sciatic nerve at 4 spots / per area. The spot size was approximately 0.2 cm^2. The output power of the laser irradiation was 30 mW per session for 60 sec/ per spot for 7 consecutive days. The energy density was 9 J/cm^2. The output of the equipment was routinely checked by the Laser Check Power Meter (Coherent, Santa Clara, CA, USA). A similar procedure was applied to the control group with sham-irradiated LLLT with the output power of laser irradiation adjusted to 0.

Mechanical Allodynia

The assessment of mechanical allodynia was performed by a MPWT which was measured by nociceptive thresholds to stimulate von Frey filaments at pre-op, post-op, 7d post-op and post-tr. The test consisted of evoking a hind paw flexion reflex with a handheld force transducer (electronic von Frey anesthesiometer, IITC Inc., CA, USA) adapted with a 0.5 mm^2

polypropylene tip. In a quiet room, the rats were placed in acrylic cages (32 × 22 × 27 cm high) with a wire grid floor for 15-30 min habituation prior to testing. The polypropylene tip was perpendicularly applied to the central area of the hind paw with sufficient force to bend the filaments into an "S" shape for 3-4 sec. The test consisted of poking a hind paw to provoke a flexion reflex followed by a clear flinch response after paw withdrawal. Testing was initiated with the filament corresponding to 20 log of force (g). The filaments were applied with a gradual increase in pressure until a withdrawal reflex response was finally detected from the animal. The response to this filament was defined if a series of weaker or stronger filaments would be tested. The weakest filament able to elicit a response was taken to be the MPWT (g). The intensity of the pressure was recorded and the final value for the response was obtained by averaging five measurements.

Assessments of Functional Recovery

The degree of recovery was monitored by evaluating the rats' walking patterns in order to obtain SFI, TFI, and PFI according to the method described by Bain et al. (Bain et al., 1989). Before the recording, a few conditioning trials were performed to accustom the animals to the track. All animals underwent preoperative walking-track analysis. Briefly, the plantar surfaces of both hind paws were wetted with red ink in order to obtain clear footprints, and they were allowed to walk along a specially designed alley (84 cm length × 8.5 cm width) lined with scaled paper. Recordings continued until five measurable footprints had been collected. The data used for calculations were taken from the footprint as follows: (1) distance from the heel to the third toe, the print length (PL); (2) distance from the first to fifth toe, the toe spread (TS); and, (3) distance from the second to the fourth toe, the intermediary toe spread (ITS). All three measurements were taken from the experimental (^{E}) and normal (^{N}) sides. Prints were then calculated using the following formulae (Bain et al., 1989): (1) SFI = -38.3 ([^{E}PL−^{N}PL]/^{N}PL) + 109.5 ([^{E}TS−^{N}TS]/^{N}TS) + 13.3 ([^{E}IT−^{N}IT]/^{N}IT) - 8.8; (2) TFI = -37.2 ([^{E}PL−^{N}PL]/^{N}PL) + 104.4 ([^{E}TS−^{N}TS]/^{N}TS) + 45.6 ([^{E}IT−^{N}IT]/^{N}IT) - 8.8; (3) PFI = 174.9 ([^{E}PL−^{N}PL]/^{N}PL) + 80.3 ([^{E}TS−^{N}TS]/^{N}TS) - 13.4. Values of these tests equal to -100 indicated total impairment of the sciatic, posterior tibial and peroneal nerves, whereas SFI, TFI and PFI oscillating around 0 were considered to reflect normal function (Bain et al., 1989).

Sciatic Nerve Obtainment and Tissue Preparations

After completing the treatments at day 14, rats were sacrificed after being deeply anaesthetized with saturated KCl (300 g/ml, i.p.), then sciatic nerve segment was harvested, which included the four ligatures as well as 1 cm of sciatic nerve proximal to the site of CCI. The biopsied nerve specimens were divided into two portions for histopathology and immunoassays. For histopathological assessments, nerve specimens randomly selected from 5 animals of each group were fixed in 10% neutral formalin, and embedded in paraffin for 12 h at room temperature. All of the biopsied nerve specimens obtained from each animal for immunoassays were immediately frozen in liquid nitrogen and stored at −80℃ for later homogenization and subsequent assay of cytokine and protein expression. The homogenization buffer was freshly prepared by adding protease inhibitor (P8340 cocktail Sigma, NY, USA) to T-PER™ Tissue Protein Extraction Reagent (Pierce Chemical Co., USA) and centrifuged for 40 min. The supernatant was extracted and stored at −80 °C.

Histopathological, Immunohistochemical and Immunofluorescent Stainings

The specimens were submitted to diafanization with xylene, then dehydrated by graded ethanol, embedded in paraffin and cut in 4-μm-thick sections longitudinally using a microtome.

Ten consecutive longitudinal resections contiguous to a maximum diameter were chosen for data collection and subsequent comparisons. Histopathologic changes were evaluated on sections stained with hematoxylin and eosin (H&E, Muto Pure Chemicals Co., Ltd., Tokyo, Japan) to determine infiltration of inflamed cells in nerves. Slides were examined by a light microscope and photographed using the Automatic Photomicrographic System PM10SP (Olympus, PA, USA). The area of inflamed cell and nerve nuclei was measured in a 200× magnification field by an ImageScope program (Aperio, Vista, CA, USA).

For immunohistochemical staining, the slides of sciatic nerve sections were first incubated overnight at 4℃ with the monoclonal mouse antibodies, including anti-HIF-1α (1:200, Thermo, CA, USA), anti-monocytes/macrophages (ED1, 1:200, Millipore, CA, USA) primary antibodies, with the polyclonal rabbit antibodies, including anti-Schwann cells (S100, 1:400, DakoCytomation, Denmark) and anti-VEGF (1:200, Abbiotec, CA, USA) primary antibodies, as well as with rabbit monoclonal anti-NGF-β (1:2500, Millipore, CA. USA) primary antibody. After washing three times in PBS, the nerve sections were then incubated with biotinylated goat anti-mouse and goat anti-rabbit IgG secondary antibody (Jackson ImmunoResearch Laboratories, Inc., West Grove, PA, USA) for 1 hour at room temperature. Following washing with phosphate buffer three times, sections were incubated with a streptavidin-horseradish peroxidase conjugate (Jackson ImmunoResearch Laboratories, Inc., West Grove, PA, USA). Finally, sections were visualized as brown precipitates yields using 3,3′-diaminobenzidine (DAB, 0.2 mg/ml, Pierce, Rockford, IL, USA) as a substrate and then counterstained with hematoxylin. Negative control sections received the same treatment without the addition of primary antibody. Slides were examined at a minimum of five sections in the more representative fields using a light microscope and then photographed. The area sizes of positive nuclear and cytoplasmic staining cells for HIF-1α, ED1, S100, VEGF and NGF were measured in a 200× magnification field using the ImageScope program (Aperio, Vista, CA, USA). Ten fields of each slide were calculated and repeated three times for statistical analysis. Results are expressed as the proportion (%) of positive immunoreactive area per total stained area.

To observe coexpression of HIF-1α with infiltrated inflammatory cells in the injured nerve, we incubated the sections with rabbit polyclonal anti-HIF-1α (1:200, Santa Cruz Biotechnology, CA, USA) and mouse monoclonal anti-monocytes/macrophages (ED1) (1:200, Millipore, CA, USA) overnight at 4°C under gentle agitation. Sections were then incubated with the respective secondary antibodies (Jackson ImmunoResearch Laboratories, Inc., West Grove, PA, USA), goat anti-rabbit IgG fluorescein-conjugated (FITC, 1:1000) and goat anti-mouse IgG rhodamine-conjugated (TRITC, 1:1000) secondary antibodies for 2 hours at room temperature. Following washing with phosphate buffer three times, sections were incubated with a streptavidin-horseradish peroxidase conjugate (Jackson ImmunoResearch Laboratories, Inc., West Grove, PA, USA). Finally, the sections were washed three times in PBS and then counterstained with 4′,6-diamidino-2-phenylindole (DAPI, Molecular Probes, Invitrogen Corporation, Carlsbad, CA, USA) to reveal cell nuclei. Images were obtained using a conventional fluorescence microscope (Fluoview X; Olympus, Tokyo, Japan). All of quantitative image analyses were assessed by two independent observers who were blinded to the origin of the sections to avoid bias from interobserver variability.

Enzyme-Linked Immunosorbent Assay

The amounts of TNF-α, IL-1β and BDNF concentrations in the supernatants were determined using the DuoSet® ELISA Development kit (R&D Systems, Minneapolis, MN, USA). Nerve extracts were incubated in 96-well plates coated with mouse anti-rat TNF-α and goat anti-rat IL-1β. After washing at each step, biotinylated anti-rat TNF-α and anti-rat IL-1β

and then streptavidin-HRP were added and incubated in accordance with the manufacturer's instructions. After washing, a NeA-Blue (Tetramethylbenzidine**)** Substrate solution (Clinical Science Products, Inc., Mansfield, MA, USA) was added to each well. The enzyme reaction was terminated by adding stop solution (2N H_2SO_4). The levels of TNF-α and IL-1β were assessed by a reader (Thermo Scientific Multiskan EX, Finland) using a 450 nm filter and normalized with an abundance of standard solution. Data were then analyzed using Ascent Software (Thermo Scientific Ascent Software, Finland) and a four-parameter logistics curve-fit. Data are expressed in pg/mg protein of duplicate samples.

Western Blot Analysis

Protein determination was performed by modified Lowry protein assays. Equal amounts of protein were loaded and separated in 10% Tris-Tricine SDS-PAGE gels. The resolved proteins were transferred onto PVDF membranes ((Millipore, Bedford, MA, USA). The membranes were blocked in 5% non-fat milk for 1 hour at room temperature, and incubated overnight at 4 °C with mouse monoclonal anti-HIF-1α (1:500, Novus Biologicals, CA, USA), rabbit polyclonal anti-VEGF antibody (1:2500, Abbiotec, CA, USA), and rabbit monoclonal anti-NGF-β (1:2500, Millipore, CA. USA) primary antibody. The blots were then incubated with the horseradish peroxidase-conjugated goat anti-mouse and anti-rabbit IgG secondary antibody (1:20000, Jackson ImmunoResearch Laboratories, Inc., West Grove, PA, USA) for 1 hour at room temperature. Signals were finally visualized using enhanced chemiluminescence detection system (Fujifilm LAS-3000 Imager, Tokyo, Japan) and the blots were exposed to X-ray films. All Western blot analyses were performed at least three times, and consistent results were obtained. Immunoreactive bands were analysed using a computer-based densitometry Gel-Pro Analyzer (version 6.0, Media Cybernetics, Inc. USA). Grey levels, obtained by densitometric analysis of immunoreactive bands, were normalized on β-actin.

Statistical Analysis

Results were averaged for each group and values were expressed as mean ± S.E.M. The data obtained from MPWT, SFI, TFI and PFI were analyzed using mixed-design, two-way repeated-measures ANOVA performed with group as a between-subjects factor and time as a within-subjects factor. The Bonferroni adjustment was examined post hoc for multiple comparisons at individual time points between groups. One-way ANOVA was performed for comparison of individual group means for assessing parametric results of histopathology and immunoassay. The Dunnett test was performed for multiple comparisons between experimental and control groups at the post-tr time point. A P value of $< .05$ was considered statistically significant. All data were analyzed using SPSS version 10.0 for Windows (SPSS Inc., IL, USA).

RESULTS

Effects of Low-Level Laser Therapy on Mechanical Allodynia

After surgery, there were significant differences in MPWT among time points in each group ($P < .0001$). MPWT was significantly decreased at post-op and 7d post-op conditions in animals that received CCI when compared with that of the pre-op condition (both were $P < 0.001$). In animals that received sham-operated CCI, MPWT of post-op compared to that of pre-op condition was significantly decreased ($P < 0.0001$), whereas there was no significant difference between the 7d post-op and pre-op condition (P=0.36). There were also significant

differences among the four groups at each time point (all were $P < 0.0001$, Figure 2A).

At the post-tr time point, there was a significant difference in MPWT compared with that of the 7d post-op condition in CL group ($P < .0001$), but there were no significant differences compared with values obtained in the CsL (P=0.59), sCL (P=0.22) and sCsL (P=0.98) groups. The significant differences in MPWT were shown among CL, CsL, sCL and sCsL groups after treatments ($P < .0001$). Significantly higher MPWT existed after LLLT treatment in CL group compared with those in CsL groups after sham-irradiated LLLT treatment ($P < .0001$). However, no significant difference was observed between sCL and sCsL groups (P=0.98).

Effects of Low-Level Laser Therapy on Functional Recovery

After surgery, there were significant differences in SFI, TFI and PFI among time points in each group. SFI, TFI and PFI values were around 0 at pre-op condition and decreased significantly after surgery in all groups ($P < .001$). SFI and TFI were still significantly decreased at 7d post-op condition in animals that received CCI when compared with those of post-op (SFI: P=0.83; TFI: P=0.99), but PFI showed significant recovery ($P < .0001$). However, in sham-operated CCI animals at 7d post-op condition, PFI values significantly recovered and approached that of the pre-surgery condition ($P = 0.99$), and SFI and TFI were significant increased compared with those of post-op conditions (both were $P < .0001$, Figure 2B-D).

At the post-tr time point, SFI, TFI and PFI values were significantly higher when compared with those of 7d post-op in CL group (SFI: P=0.001; TFI: P=0.003; PFI=0.03), but no significant differences were found in CsL (SFI: P=1.0; TFI: P=0.73; PFI: P=1.0). SFI, TFI and PFI values in sCL and sCsL groups showed no significant difference from pre-op level (all were $P > .05$). Significant differences in SFI, TFI and PFI were shown among CL, CsL, sCL and sCsL groups (all were $P < .0001$). Significantly higher values of SFI, TFI and PFI existed after LLLT treatment in CL group compared with those of sham-irradiation treatment in CsL groups (SFI: P=0.001; TFI: P=0.004; PFI: P=0.002).

Effects of Low-Level Laser Therapy on Inflammation and Cytokines

The results of H&E study showed there was pronounced infiltration of immune cells at the site of CCI injury as compared with the site of sham-operated CCI (Figure 3A, 3B, 3C, 3D). The percentages of nuclei in nerve contents were significantly different among the four groups ($P < .0001$). The percentage of nuclei was significantly decreased and showed less inflammation and cell infiltration in CL groups when compared with CsL group (Figure 3G). Similar results were found for ED1 immunoreactivity which showed significant increases in CsL group, but was reduced in CL group (Figure 3E, 3F and 3H).

TNF-α and IL-1β of the sciatic nerve contents were significantly different among the four groups (both were $P < .0001$). There were significantly higher levels of TNF-α and IL-1β in CsL groups in comparison with those of sCsL and sCL groups (both were $P < .0001$). No significant differences were observed between sCL and sCsL groups (P=1.0). There was a significant reduction of these cytokines in the CL group when compared with CsL groups ($P < .0001$), but no significant difference was found when compared with those of sCL (TNF-α: P=0.29; IL-1β: P=0.39) or sCsL (TNF-α: P=0.33; IL-1β: P=0.28) groups (Figure 4).

Effects of Low-Level Laser Therapy on HIF-1 α

The expressions of HIF-1α immunoreactivity in sciatic nerves were significantly different among the four groups ($P < .0001$). The results showed there were sparse HIF-1α-positive cells in sCL and sCsL groups (Figure 5A, 5B) and no significant differences were found among

these groups (both were $P > .05$, Figure 5G). In the CsL group, overexpression of HIF-1α immunoreactivity was observed and localized in both the nucleus and cytoplasm of the injured samples at higher-power magnification (Figure 5C). The accumulation of HIF-1α-positive cells was decreased significantly in CL group when compared with CsL group (P=0.006, Figure 5D). Double staining with HIF-1α and ED1 showed the ED1 immunoreactive cells which were morphologically consistent with macrophages, mainly by inflammatory infiltration of the inflamed nerve coexpressed by the specific HIF-1α immunoreactivity. The number of double positive cells was decreased in CL groups when compared with those in CsL group (Figure 5E and 5J). The observed HIF-1α expressions were further supported at the protein level assay by Western blotting. The levels of HIF-1α in sciatic nerve was shown as gray density percentages (normalized on β-actin) in the form of a representative Western blotting (Figure 6H). The protein levels of HIF-1α in sciatic nerve contents were significantly different among the four groups ($P < .0001$). No significant differences were observed between sCL and sCsL groups ($P > .05$). Significantly higher levels of HIF-1α level were found in CsL groups in comparison with those of CL, sCsL and sCL groups (all were $P < .0001$). The protein levels of HIF-1α was significantly decreased in CL group in comparison with CsL groups (P=0.006) and approximated the levels of sCL control group (P=0.064).

Effects of Low-Level Laser Therapy on VEGF, NGF and Schwann Cells

At day 14 after CCI, the constitutive expressions of VEGF and NGF in sciatic nerves were significantly different among the four groups (VEGF: $P < .0001$; NGF: P=0.003). There were no significant differences of VEGF and NGF expression between sCL and sCsL groups (both were $P > .05$). After CCI, the expressions of these factors in the injured sciatic nerve were slightly increased in CsL group as shown in Figures 6A and 6D, but the difference was of non-significant when compared with those of sCsL groups (NGF: P=0.9; VEGF: P=0.22). As expected, our results demonstrated that there were significant increases of VEGF and NGF in CL groups compared with those in CsL group (VEGF: P=0.009; NGF: P=0.002, Figure 6B, 6C, 6E and 6F). Furthermore, as demonstrated in Figure 6I and 6J, the observed VEGF and NGF immunoreactive expressions could be further supported at the protein level by Western blotting. The protein levels of VEGF and NGF in sciatic nerve contents were also significantly different among the four groups (VEGF: $P < .0001$; NGF: $P < .0001$). No significant differences were observed between sCL and sCsL groups (both were P=1.0). The protein levels of VEGF and NGF in CsL group also showed a slight elevation over 14 days after CCI surgery but the calculation was not significant when compared with those of sCsL groups (NGF: P=0.18; VEGF: P=0.07). There were significant increases of levels of VEGF and NGF in CL group when compared with those of CsL groups (VEGF: P=0.009; NGF: P=0.002). Using S100 immunohistochemistry for Schwann cells, the S100 expression was decreased in injured nerve in CsL group (Figure 6G), but increased in CL group (Figure 6H). The S100 immunoreactivity in sciatic nerve contents was also significantly different among the four groups ($P < .0001$). There was a significant decrease in S100 expression in CsL group when compared with values seen in CL (P=0.005), sCL (P=0.035) and sCsL (P=0.027) groups (Figure 6I).

DISCUSSION

In the current study, we demonstrated that 660nm-GaAlAs-LLLT at a dose of 9 J/cm^2 significantly reduced neuropathic allodynia in CCI rats. Our results are similar to those of previous reports demonstrating that Nd: YAG laser-applied rats that received soft tissue surgery had significantly higher nociceptive thresholds of the hind paw compared with the controls on

the 7th postoperative day (Kara et al., 2010) and 830 nm-wavelength LLLT at doses of 4 and 8 J/cm^2 over the surgical incision on the 3rd postoperative day was effective in reducing pain in rats with sciatic nerve compression using catgut thread (Bertolini et al., 2011). In clinical studies of carpal tunnel syndrome, there was a significant improvement in neuropathy-induced pain and delay of nerve conduction in patients undergoing LLLT over the carpal tunnel area (Elwakil et al., 2007) (Shooshtari et al., 2008).

Pain due to inflammation is characteristic of neuropathy (Sommer and Kress, 2004, Sommer and Schäfers, 2004, Li et al., 2011, Liou et al., 2011). As previously described, mediators released from infiltrated cells, such as TNF-α and IL-1, have been implicated directly in neuropathic pain, chronic hyperalgesia, and allodynia (Wagner and Myers, 1996, DeLeo et al., 1997). Based on our observations from CCI rats in this study, the infiltration cells and the protein levels of TNF-α and IL-1β in damaged nerves were significantly increased in the control group. It seems that the contribution of inflammation and pro-inflammatory cytokines to neuropathic pain were predominantly observed in the late postinjury phases. Our results are further supported by a recent study with CCI rat model which showed reduction of MPWT was correlated with increases of TNF-α and IL-1β gene expression in sciatic nerve (Okamoto et al., 2001). Our results also demonstrated the infiltration of inflamed cells and the release of proinflammatory cytokines were significantly reduced after LLLT in comparison with the sham-irradiated controls. This result is similar to findings of previous studies with a rat model of carrageenan-induced inflammation (Albertini et al., 2008, Boschi et al., 2008). Therefore, the alleviation of neuropathic pain treated with LLLT in this study was probably due to the reduction of inflammation and pro-inflammatory cytokines of injured nerve tissue.

SFI, TFI and PFI described by Bain et al. (Bain et al., 1989) are well-established and are useful techniques for quantitatively assessing a rat's lower limb deficits and determining lesion-induced changes in function in sciatic nerve and its muscular branches in the rat. Therefore, footprints were obtained after CCI for evaluation of functional locomotor recovery by means of the SFI, TFI and PFI in this study. Our results showed that the SFI, TFI and PFI were significantly affected by CCI at proximal stump of sciatic nerve. Probably owing to impairment of sciatic nerve function and pain induced by CCI, prints were found to be abnormal with evidence of toe dragging and a more "slurred" print. The use of LLLT significantly promoted functional recovery as evidenced by increases in the SFI, TFI and PFI. These results are consistent with the findings of a previous study that demonstrated LLLT was effective in promoting early functional recovery as indicated by the SFI (Barbosa et al., 2010).

A nerve constriction injury produces histopathologic changes similar to the manner in which a ischemic nerve injury can produce hyperesthesia when it causes Wallerian degeneration (Myers et al., 1993). These data suggest that the nerve ischemia itself may play an important role in the development of the hyperesthesia and allodynia induced by nerve CCI (Myers et al., 1993). In response to ischemic damage in nerve, involvement of the ischemia-related gene HIF-1α has been reported (Goldenberg-Cohen et al., 2009). HIF-1 has dual effects and can induce either cell survival or cell death (Semenza, 2000). Accumulation of HIF-1α protein and increase of HIF-1 activity have been found to exist following inflammation, probably induced by pro-inflammatory cytokines, i.e., IL-1 and TNF-α (Hellwig-Burgel et al., 2005, Dehne and Brune, 2009, Chou et al., 2011). HIF-1 also existed in macrophage to optimize its innate immunity, control pro-inflammatory gene expression and influence cell migration (Dehne and Brune, 2009). Our previous findings showed pain and infiltration of inflamed cells can be reduced by reducing HIF-1α protein accumulation in an arthritic animal model (Chou et al., 2011). An *in vitro* study demonstrated that impaired neurons can be rescued to promote neurogenesis by stabilizing HIF-1α (Milosevic et al., 2009). Therefore,

stabilization of HIF-1α protein expression as a regulator of gene expression in tissues is required for the establishment of normal physiological systems (Semenza, 2000). The results of this study demonstrated that the accumulation of HIF-1α in damaged nerve tissues was prominent in response to CCI and were suppressed after LLLT. LLLT also reduced HIF-1α expression in macrophages which coordinate chronic inflammation and immune responses. Our results are consistent with a recent study which employed a mouse infection model to investigate wound healing and demonstrated that untreated lesions showed high immunoreactivity for HIF-1α, whereas little immunoreactivity could be detected in laser-treated lesions (Ferreira et al., 2009). We postulate that this finding may help to explain the ability of laser radiation to eliminate HIF-1α accumulation and then stabilize its activity, thereby stimulating aerobic cell metabolism, accelerating tissue repair and promoting functional recovery.

Vascular alterations of peripheral nerves occurring after injury are well described. Angiogenesis is an essential component of nerve re-growth, and regeneration of the endoneural vasculature precedes the outgrowth of axons from the proximal stump (Hoke, 2006, Webber and Zochodne, 2010). It is thought that VEGF, a potent growth factor for angiogenesis, also plays an important role in proliferation of Schwann cells, nerve repair and motor performance (Hobson et al., 2000, Pereira Lopes et al., 2011). Increased angiogenesis primarily takes place in metabolically altered or in injured peripheral nerves (Samii et al., 1999). Moreover, stabilization of HIF-1α in a mouse with diabetes enhances wound healing and increases VEGF production (Mace et al., 2007). Our findings demonstrated that CCI rats with sensory neuropathy expressed VEGF in sciatic nerves. LLLT could further facilitate a prominent increase of VEGF immunoreactivity compared with that obtained by sham-irradiation. This effect was probably achieved through the stabilization of HIF-1α protein activity. In a study which revealed similar findings to those of the present investigation it was shown that LLLI could stimulate proliferation, increase VEGF secretion and facilitate myogenic differentiation of bone marrow-derived mesenchymal stem cells (Hou et al., 2008), indicating that LLLT can accelerate the healing process of tissues by stimulating VEGF.

NGF may act positively on the regeneration and growth of axonal processes to promote the survival and integrity of sensory neurons and reverse distinct morphological and sensory deficits and degeneration of myelin (Apfel et al., 1994). NGF also increases the levels of VEGF in normal neural cells (Calza et al., 2001) and stimulates angiogenesis in animal models under ischemic condition (Turrini et al., 2002). Local administration of anti-NGF serum can block sprouting of collateral nerve fiber after sciatic nerve CCI in rats (Ro et al., 1998). Improvement of sensory neuropathy and nerve fiber morphology could also be achieved by application of NGF (Unger et al., 1998). In accordance with these previous findings, our results showed that the elevation of NGF protein by LLLT was greater than that found in animals treated with sham-irradiation. Moreover, in this study, an increase of S100 immunoreactivity was also found after LLLT, indicating an increase in Schwann cells and these changes may be attributed to improvement of functional motor status measured by SFI, TFI and PFI. Therefore, improvement of neural function could also be achieved by application of LLLT which can increase protein levels of NGF and VEGF to repair the myelin sheath in the injured nerve tissues.

CONCLUSIONS

The aim of this study was to analyze the influence of injured nerve irradiation using a 660-nm Ga-Al-As diode laser on the neurorehabilitation of CCI sciatic nerves. The behavioral evaluation of rats indicated that LLLT on CCI nerve tissues yielded much better recovery with regard to motor function, pain behavior and histomorphometry than that achieved by sham-irradiation. LLLT also reduced the protein levels of pro-inflammatory cytokines and HIF-1α accumulation, and elevated levels of VEGF and NGF of the nerve tissue. These results support our postulation that LLLT applied transcutaneously to the CCI nerve can suppress inflammation-induced TNF-α, IL-1β and HIF-1α accumulation to control the neuropathic pain and elevate the levels of VEGF and NGF in injured nerve thereby promoting functional recovery and nerve regeneration. These results also indicate that the LLLT can modulate HIF-1α activity and may represent a novel therapeutic approach as a clinically applicable modality for improvement of tissue hypoxia/ischemia in nerve entrapment neuropathy as well as for acceleration of the reinnervation rate of regenerated nerves, which may lead to sufficient morphologic and functional recovery of the peripheral nerve.

ACKNOWLEDGEMENTS

The authors gratefully acknowledge the pathological and technical expertise of Mr. Shih-Chung Chen in this study. This study was supported by a grant from China Medical University (CMU99-TC-23), Taiwan.

REFERENCES

Albertini R, Villaverde AB, Aimbire F, Bjordal J, Brugnera A, Mittmann J, Silva JA, Costa M (Cytokine mRNA expression is decreased in the subplantar muscle of rat paw subjected to carrageenan-induced inflammation after low-level laser therapy. Photomed Laser Surg 26:19-24.2008).

Albertini R, Villaverde AB, Aimbire F, Salgado MA, Bjordal JM, Alves LP, Munin E, Costa MS (Anti-inflammatory effects of low-level laser therapy (LLLT) with two different red wavelengths (660 nm and 684 nm) in carrageenan-induced rat paw edema. J Photochem Photobiol B 89:50-55.2007).

Apfel SC, Arezzo JC, Brownlee M, Federoff H, Kessler JA (Nerve growth factor administration protects against experimental diabetic sensory neuropathy. Brain Res 634:7-12.1994).

Bain JR, Mackinnon SE, Hunter DA (Functional evaluation of complete sciatic, peroneal, and posterior tibial nerve lesions in the rat. Plast Reconstr Surg 83:129-138.1989).

Barbosa RI, Marcolino AM, de Jesus Guirro RR, Mazzer N, Barbieri CH, de Cassia Registro Fonseca M (Comparative effects of wavelengths of low-power laser in regeneration of sciatic nerve in rats following crushing lesion. Lasers Med Sci 25:423-430.2010).

Baron R (Peripheral neuropathic pain: from mechanisms to symptoms. Clin J Pain 16:S12-20.2000).

Bennett GJ, Xie YK (A peripheral mononeuropathy in rat that produces disorders of pain sensation like those seen in man. Pain 33:87-107.1988).

Bertolini GR, Artifon EL, Silva TS, Cunha DM, Vigo PR (Low-level laser therapy, at 830 nm, for pain reduction in experimental model of rats with sciatica. Arq Neuropsiquiatr 69:356-359.2011).

Boschi ES, Leite CE, Saciura VC, Caberlon E, Lunardelli A, Bitencourt S, Melo DA, Oliveira JR (Anti-Inflammatory effects of low-level laser therapy (660 nm) in the early phase in carrageenan-induced pleurisy in rat. Lasers Surg Med 40:500-508.2008).

Byrnes KR, Wu X, Waynant RW, Ilev IK, Anders JJ (Low power laser irradiation alters gene expression of olfactory ensheathing cells in vitro. Lasers Surg Med 37:161-171.2005).

Calza L, Giardino L, Giuliani A, Aloe L, Levi-Montalcini R (Nerve growth factor control of neuronal expression of angiogenetic and vasoactive factors. Proc Natl Acad Sci U S A 98:4160-4165.2001).

Chou LW, Wang J, Chang PL, Hsieh YL (Hyaluronan modulates accumulation of hypoxia-inducible factor-1 alpha, inducible nitric oxide synthase, and matrix metalloproteinase-3 in the synovium of rat adjuvant-induced arthritis model. Arthritis Res Ther 13:R90.2011).

Dehne N, Brune B (HIF-1 in the inflammatory microenvironment. Exp Cell Res 315:1791-1797.2009).

DeLeo JA, Colburn RW, Rickman AJ (Cytokine and growth factor immunohistochemical spinal profiles in two animal models of mononeuropathy. Brain Res 759:50-57.1997).

Elwakil TF, Elazzazi A, Shokeir H (Treatment of carpal tunnel syndrome by low-level laser versus open carpal tunnel release. Lasers Med Sci 22:265-270.2007).

Ferreira MC, Gameiro J, Nagib PR, Brito VN, Vasconcellos Eda C, Verinaud L (Effect of low intensity helium-neon (HeNe) laser irradiation on experimental paracoccidioidomycotic wound healing dynamics. Photochem Photobiol 85:227-233.2009).

Fraisl P, Aragones J, Carmeliet P (Inhibition of oxygen sensors as a therapeutic strategy for ischaemic and inflammatory disease. Nat Rev Drug Discov 8:139-152.2009).

539 Gigo-Benato D, Geuna S, Rochkind S (Phototherapy for enhancing peripheral nerve repair: a
540 review of the literature. Muscle Nerve 31:694-701.2005).
541 Gigo-Benato D, Russo TL, Tanaka EH, Assis L, Salvini TF, Parizotto NA (Effects of 660 and
542 780 nm low-level laser therapy on neuromuscular recovery after crush injury in rat sciatic
543 nerve. Lasers Surg Med 42:673-682.2010).
544 Goldenberg-Cohen N, Dadon-Bar-El S, Hasanreisoglu M, Avraham-Lubin BC,
545 Dratviman-Storobinsky O, Cohen Y, Weinberger D (Possible neuroprotective effect of
546 brimonidine in a mouse model of ischaemic optic neuropathy. Clin Experiment Ophthalmol
547 37:718-729.2009).
548 Hellwig-Burgel T, Stiehl DP, Wagner AE, Metzen E, Jelkmann W (Review: hypoxia-inducible
549 factor-1 (HIF-1): a novel transcription factor in immune reactions. J Interferon Cytokine Res
550 25:297-310.2005).
551 Hobson MI, Green CJ, Terenghi G (VEGF enhances intraneural angiogenesis and improves
552 nerve regeneration after axotomy. J Anat 197 Pt 4:591-605.2000).
553 Hoke A (Neuroprotection in the peripheral nervous system: rationale for more effective
554 therapies. Arch Neurol 63:1681-1685.2006).
555 Hou JF, Zhang H, Yuan X, Li J, Wei YJ, Hu SS (In vitro effects of low-level laser irradiation
556 for bone marrow mesenchymal stem cells: proliferation, growth factors secretion and
557 myogenic differentiation. Lasers Surg Med 40:726-733.2008).
558 Kara C, Suleyman H, Tezel A, Orbak R, Cadirci E, Polat B, Kara I (Evaluation of pain levels
559 after Nd: YAG laser and scalpel incisions: an experimental study in rats. Photomed Laser Surg
560 28:635-638.2010).
561 Kingery WS, Castellote JM, Wang EE (A loose ligature-induced mononeuropathy produces
562 hyperalgesias mediated by both the injured sciatic nerve and the adjacent saphenous nerve.
563 Pain 55:297-304.1993).
564 Li F, Fang L, Huang S, Yang Z, Nandi J, Thomas S, Chen C, Camporesi E (Hyperbaric
565 Oxygenation Therapy Alleviates Chronic Constrictive Injury-Induced Neuropathic Pain and
566 Reduces Tumor Necrosis Factor-Alpha Production. Anesth Analg.2011).
567 Liou JT, Liu FC, Mao CC, Lai YS, Day YJ (Inflammation confers dual effects on nociceptive
568 processing in chronic neuropathic pain model. Anesthesiology 114:660-672.2011).
569 Mace KA, Yu DH, Paydar KZ, Boudreau N, Young DM (Sustained expression of Hif-1alpha in
570 the diabetic environment promotes angiogenesis and cutaneous wound repair. Wound Repair
571 Regen 15:636-645.2007).
572 Milosevic J, Adler I, Manaenko A, Schwarz SC, Walkinshaw G, Arend M, Flippin LA, Storch
573 A, Schwarz J (Non-hypoxic stabilization of hypoxia-inducible factor alpha (HIF-alpha):
574 relevance in neural progenitor/stem cells. Neurotox Res 15:367-380.2009).
575 Myers RR, Yamamoto T, Yaksh TL, Powell HC (The role of focal nerve ischemia and
576 Wallerian degeneration in peripheral nerve injury producing hyperesthesia. Anesthesiology
577 78:308-316.1993).
578 Okamoto K, Martin DP, Schmelzer JD, Mitsui Y, Low PA (Pro- and anti-inflammatory
579 cytokine gene expression in rat sciatic nerve chronic constriction injury model of neuropathic
580 pain. Exp Neurol 169:386-391.2001).
581 Pereira Lopes FR, Lisboa BC, Frattini F, Almeida FM, Tomaz MA, Matsumoto PK, Langone F,
582 Lora S, Melo PA, Borojevic R, Han SW, Martinez AM (Enhancement of sciatic-nerve
583 regeneration after VEGF gene therapy. Neuropathol Appl Neurobiol.2011).
584 Ro LS, Chen ST, Tang LM (Extent of collateral sprouting of intact nerve fibers in rats depends
585 on the local availability of nerve growth factor. J Formos Med Assoc 97:247-251.1998).
586 Rochkind S (Phototherapy in peripheral nerve regeneration: From basic science to clinical

study. Neurosurg Focus 26:E8.2009).
Rochkind S, Geuna S, Shainberg A (Chapter 25: Phototherapy in peripheral nerve injury: effects on muscle preservation and nerve regeneration. Int Rev Neurobiol 87:445-464.2009).
Samii A, Unger J, Lange W (Vascular endothelial growth factor expression in peripheral nerves and dorsal root ganglia in diabetic neuropathy in rats. Neurosci Lett 262:159-162.1999).
Semenza GL (HIF-1: mediator of physiological and pathophysiological responses to hypoxia. J Appl Physiol 88:1474-1480.2000).
Shooshtari SM, Badiee V, Taghizadeh SH, Nematollahi AH, Amanollahi AH, Grami MT (The effects of low level laser in clinical outcome and neurophysiological results of carpal tunnel syndrome. Electromyogr Clin Neurophysiol 48:229-231.2008).
Sommer C, Kress M (Recent findings on how proinflammatory cytokines cause pain: peripheral mechanisms in inflammatory and neuropathic hyperalgesia. Neurosci Lett 361:184-187.2004).
Sommer C, Schäfers M (Mechanisms of neuropathic pain: the role of cytokines. Drug Discovery Today: Disease Mechanisms 1:441-448.2004).
Takeda K, Ichiki T, Narabayashi E, Inanaga K, Miyazaki R, Hashimoto T, Matsuura H, Ikeda J, Miyata T, Sunagawa K (Inhibition of prolyl hydroxylase domain-containing protein suppressed lipopolysaccharide-induced TNF-alpha expression. Arterioscler Thromb Vasc Biol 29:2132-2137.2009).
Turrini P, Gaetano C, Antonelli A, Capogrossi MC, Aloe L (Nerve growth factor induces angiogenic activity in a mouse model of hindlimb ischemia. Neurosci Lett 323:109-112.2002).
Unger JW, Klitzsch T, Pera S, Reiter R (Nerve growth factor (NGF) and diabetic neuropathy in the rat: morphological investigations of the sural nerve, dorsal root ganglion, and spinal cord. Exp Neurol 153:23-34.1998).
Wagner R, Myers RR (Endoneurial injection of TNF-alpha produces neuropathic pain behaviors. Neuroreport 7:2897-2901.1996).
Webber C, Zochodne D (The nerve regenerative microenvironment: early behavior and partnership of axons and Schwann cells. Exp Neurol 223:51-59.2010).
Zimmermann M (Ethical guidelines for investigations of experimental pain in conscious animals. Pain 16:109-110.1983).
Zimmermann M (Pathobiology of neuropathic pain. Eur J Pharmacol 429:23-37.2001).

Legends of Figures

Figure 1. Experimental design of the sequence of events for the entire course of the experiment. Evaluations include measurements of mechanical paw withdrawal threshold (MPWT), sciatic, tibial and peroneal functional indexes (SFI, TFI and PFI) at the periods before surgery (pre-op), immediately after surgery (post-op), 7 days after surgery (7d post-op) and after treatment (post-tr) in the chronic constriction injury (CCI) animals treated with LLLT (CL group) and sham-irradiation (CsL group) as well as in the sham-operated CCI animals treated with LLLT (sCL group) and sham-irradiation (sCsL group). After the final treatment, the animals were sacrificed for histology, immunohistochemistry (IHC), immunofluorescence (IFC), Western blotting (WB) and ELISA assays. Solid and dotted lines denote the CCI and sham-operation on the animals sciatic nerve, respectively. Solid and dotted borders of columns denote the LLLT and sham-irradiation on the animals' sciatic nerve, respectively.

Figure 2. Assessments of mechanical allodynia and functional recovery. Data were calculated before surgery (pre-op), immediately after surgery (post-op), 7 days after surgery (7d post-op) and after treatment (post-tr) in the chronic constriction injury (CCI) animals treated with LLLT (CL group) and sham-irradiation (CsL group) as well as in the sham-operated CCI animals treated with LLLT (sCL group) and sham-irradiation (sCsL group). Each value represents the mean ± SEM in mechanical paw withdrawal threshold (MPWT) (A), sciatic, tibial and peroneal functional indexes (SFI, TFI and PFI) (B-D). There were no significant differences in any of the data between sCL and sCsL groups. After LLLT, the MPWT, SFI, TFI and PFI were significantly increased when compared with those that received sham-irradiated LLLT. # indicates there were significant differences among the four groups ($P < .05$). * indicates there was a significant differences between CL and CsL groups ($P < .05$).

Figure 3. Assessments of inflammation in sciatic nerves by H&E staining and ED1 immunohistochemistry. Representative sections of the sciatic nerves obtained from chronic constriction injury (CCI) animals treated with LLLT (CL group) and sham-irradiation (CsL group) as well as in the sham-operated CCI animals treated with LLLT (sCL group) and sham-irradiation (sCsL group). A-D indicate H&E staining for histopathology of sciatic nerves. In rats of sCL and sCsL groups, the nerve tissues show normal histological appearance (A, B). In rats of CsL group, there was even greater and massive inflammatory cells infiltration in injured nerves (C). However, in rats of CL group, there was less infiltration in the nerves and less accumulation of inflamed cells (D). For ED1 immunohistochemistry, there was more ED1 immunoreactivity (DAB-brown) in CsL group (E) than that in CL group (F). The quantitative analysis of H&E and immunostaining for inflamed cells and ED1 are showed in F and G, respectively. # indicates a statistically significant difference ($P < .05$) when data for CsL group were compared with those of CL, sCsL and sCL groups and * indicates a significant difference ($P < .05$) when data for CL groups were compared with data from CsL, sCL, sCsL groups. A scale bar indicates 100 μm. Original magnification was ×400.

Figure 4. Results of TNF-α and IL-1β protein levels in the sciatic nerve. The levels of TNF-α (A) and IL-1β (B) proteins were measured by ELISA in the sciatic nerves removed from the chronic constriction injury (CCI) animals treated with LLLT (CL group) and sham-irradiation (CsL group) as well as in the sham-operated CCI animals treated with LLLT (sCL group) and sham-irradiation (sCsL group). # indicates a statistically significant difference ($P < .05$) between CsL group and sCsL and sCL groups. # indicates a significant difference ($P < .05$) between CL groups and CsL groups.

Figure 5. Results of HIF-1α expression in the sciatic nerve. Representative sections of the sciatic nerves obtained from chronic constriction injury (CCI) animals treated with LLLT (CL group) and sham-irradiation (CsL group) as well as in the sham-operated CCI animals treated with LLLT (sCL group) and sham-irradiation (sCsL group). In rats of sCL and sCsL groups, nerve tissue showed low HIF-1α expression (A, B). In rats of CsL group, there was even greater and massive HIF-1α accumulation (DAB-brown) in injured nerves (C). But in rats of CL group, there was less HIF-1α accumulation in nerves (D). Double staining with HIF-1α (FITC-green), ED1 (TRITC-red) and DAPI (blue) by immunofluorescence showed there was more co-expression of HIF-1α and ED1 (light red) in CsL groups (E) than that in CL groups (F). The quantitative analysis of HIF-1α immunoreactivity for positive stained area is shown in G. The protein levels of HIF-1α immunoblotting were significantly increased in CsL and decreased in CL group (H). # indicates a statistically significant difference ($P < .05$) between CsL group and sCsL and sCL groups. * indicates a significant difference ($P < .05$) for CL compared with CsL groups. A scale bar indicates 100 μm. Original magnification was ×400.

Figure 6. Results of NGF, VEGF and S100 expressions in the sciatic nerve. Representative sections of the sciatic nerves obtained from chronic constriction injury (CCI) animals treated with LLLT (CL group) and sham-irradiation (CsL group) as well as in the sham-operated CCI animals treated with LLLT (sCL group) and sham-irradiation (sCsL group). In rats of sCL and sCsL groups, nerve tissue showed low NGF and VEGF expression (data not shown). In rats of CsL group, there was slightly increased NGF (A) and VEGF (B) expression in injured nerves compared with those in sham-operated CCI nerves. But in rats of CL group, the nerves expressed more NGF and VEGF accumulation (D). For coexpression of ED1 and HIF-1α immunofluorescence, there were more coexpressions (shown in light red) in CsL groups (E) than those in CL groups (F). The quantitative analysis of HIF-1α immunoreactivity for positive stained area is shown in G. The protein levels of HIF-1α immunoblotting showed a significant increase in CsL and a decrease in CL group (H). # indicates a statistically significant difference ($P < .05$) for CsL groups compared with CL, sCsL and sCL groups, and * indicates a significant difference between CL group and CsL, sCsL and sCL groups ($P < .05$). A scale bar indicates 100 μm. Original magnification was ×400.

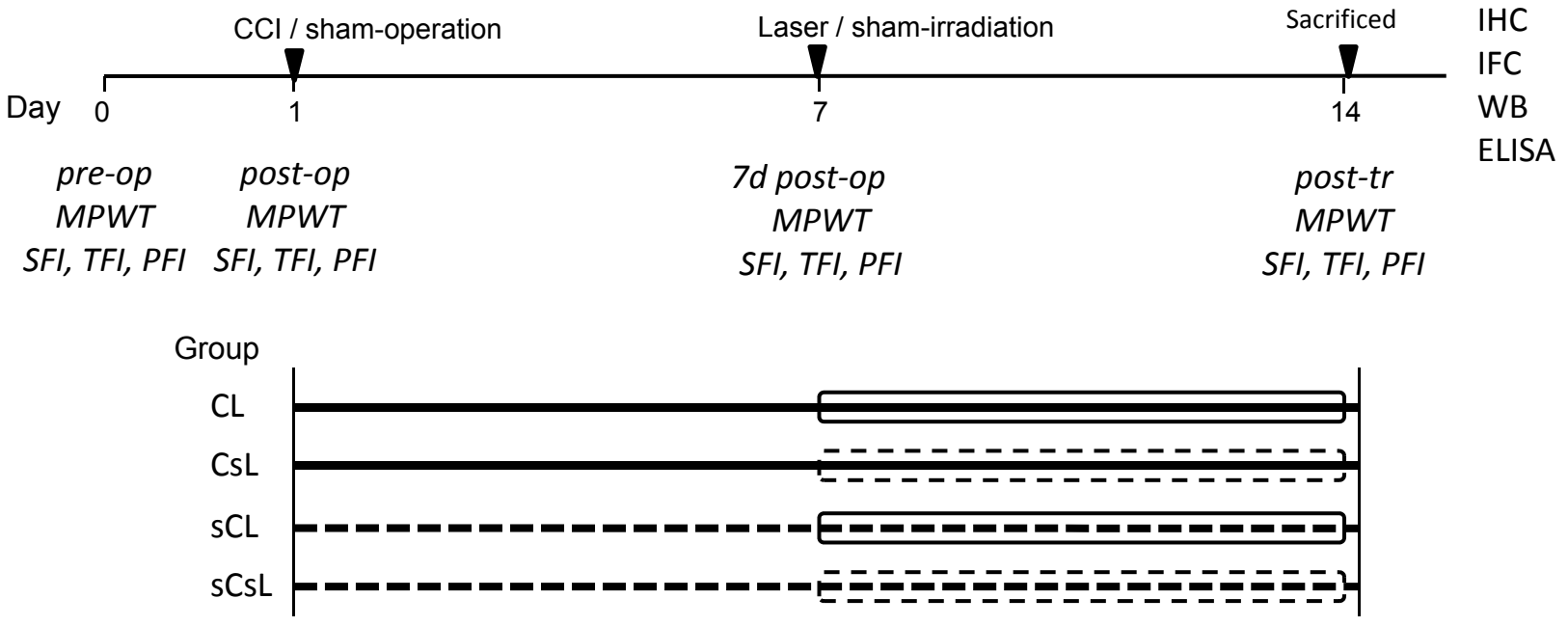
CCI / sham-operation
Laser / sham-irradiation
Sacrificed
IHC
IFC
WB
ELISA
Day
0
1
7
14
pre-op
MPWT
SFI, TFI, PFI
post-op
MPWT
SFI, TFI, PFI
7d post-op
MPWT
SFI, TFI, PFI
post-tr
MPWT
SFI, TFI, PFI
Group
CL
CsL
sCL
sCsL

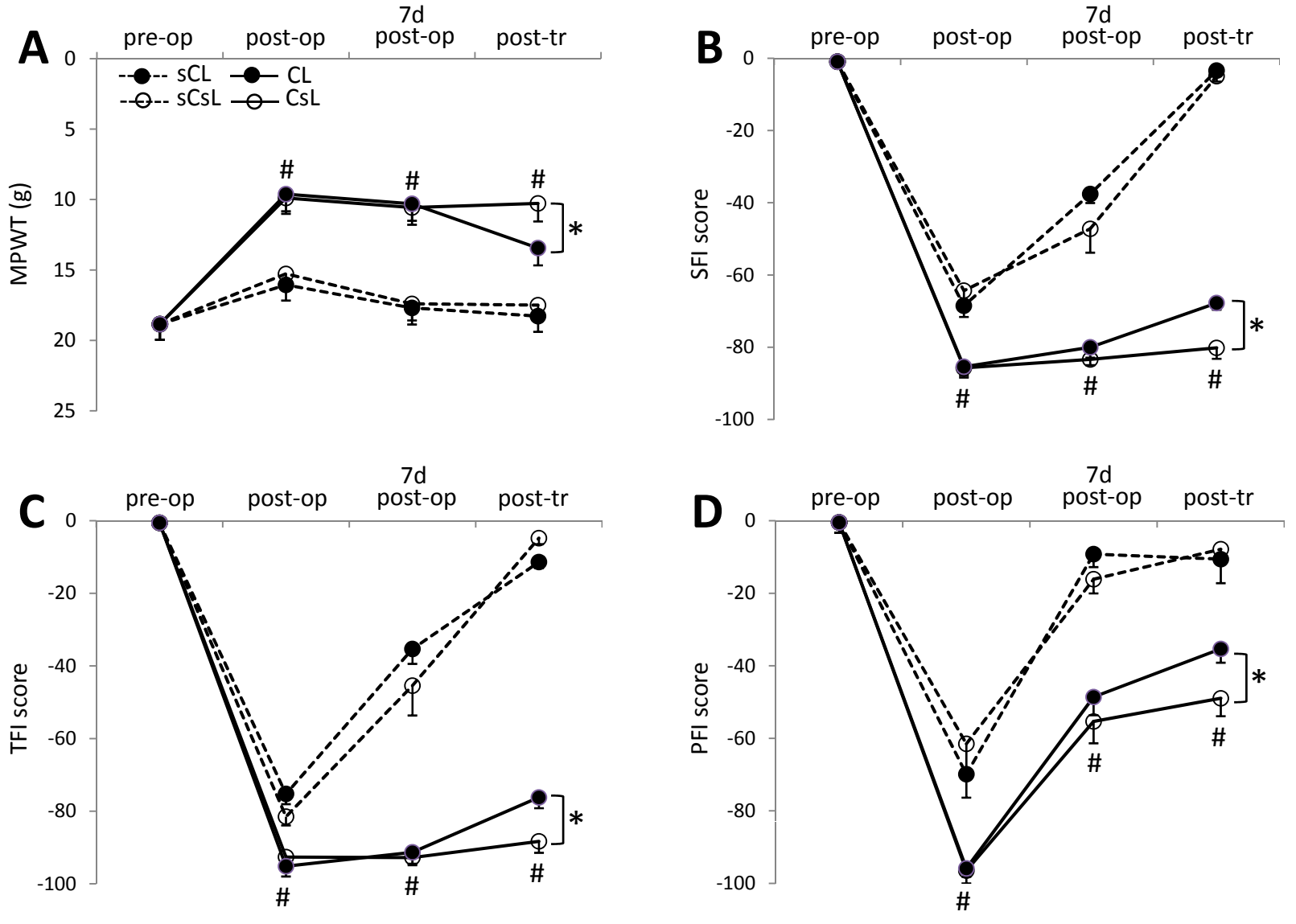
A
pre-op
post-op
7d post-op
post-tr
sCL
CL
sCsL
CsL
MPWT (g)
0
5
10
15
20
25
#
*
B
SFI score
-20
-40
-60
-80
-100
C
TFI score
D
PFI score

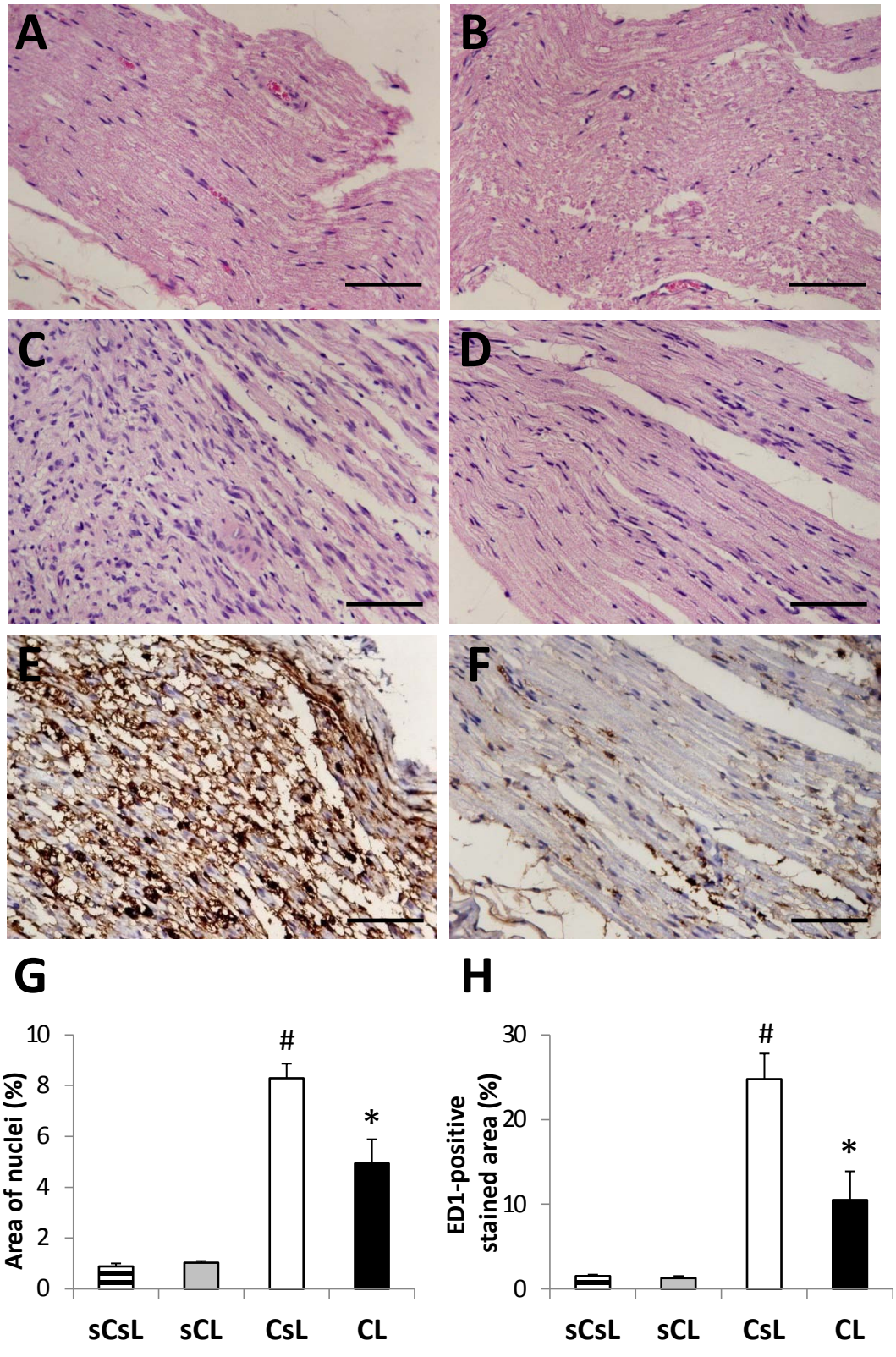
A
B
C
D
E
F
G
Area of nuclei (%)
10
8
6
4
2
0
#
*
sCsL
sCL
CsL
CL
H
ED1-positive stained area (%)
30
20
10
0
#
*
sCsL
sCL
CsL
CL

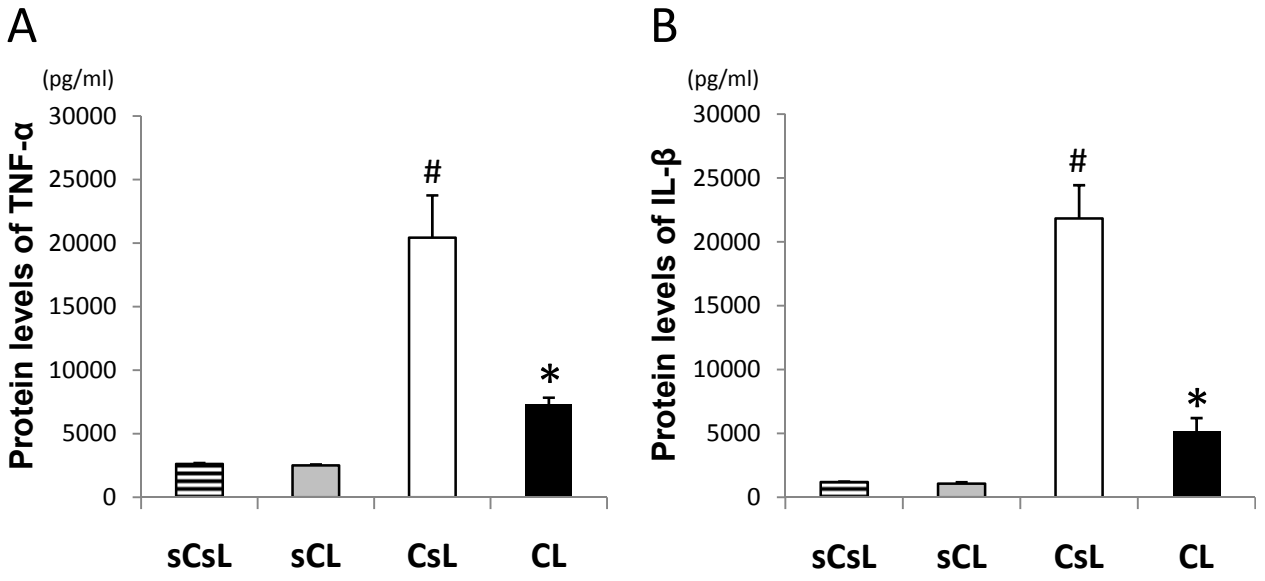

Figure 4. Results of TNF-α and IL-1β protein levels in the sciatic nerve.

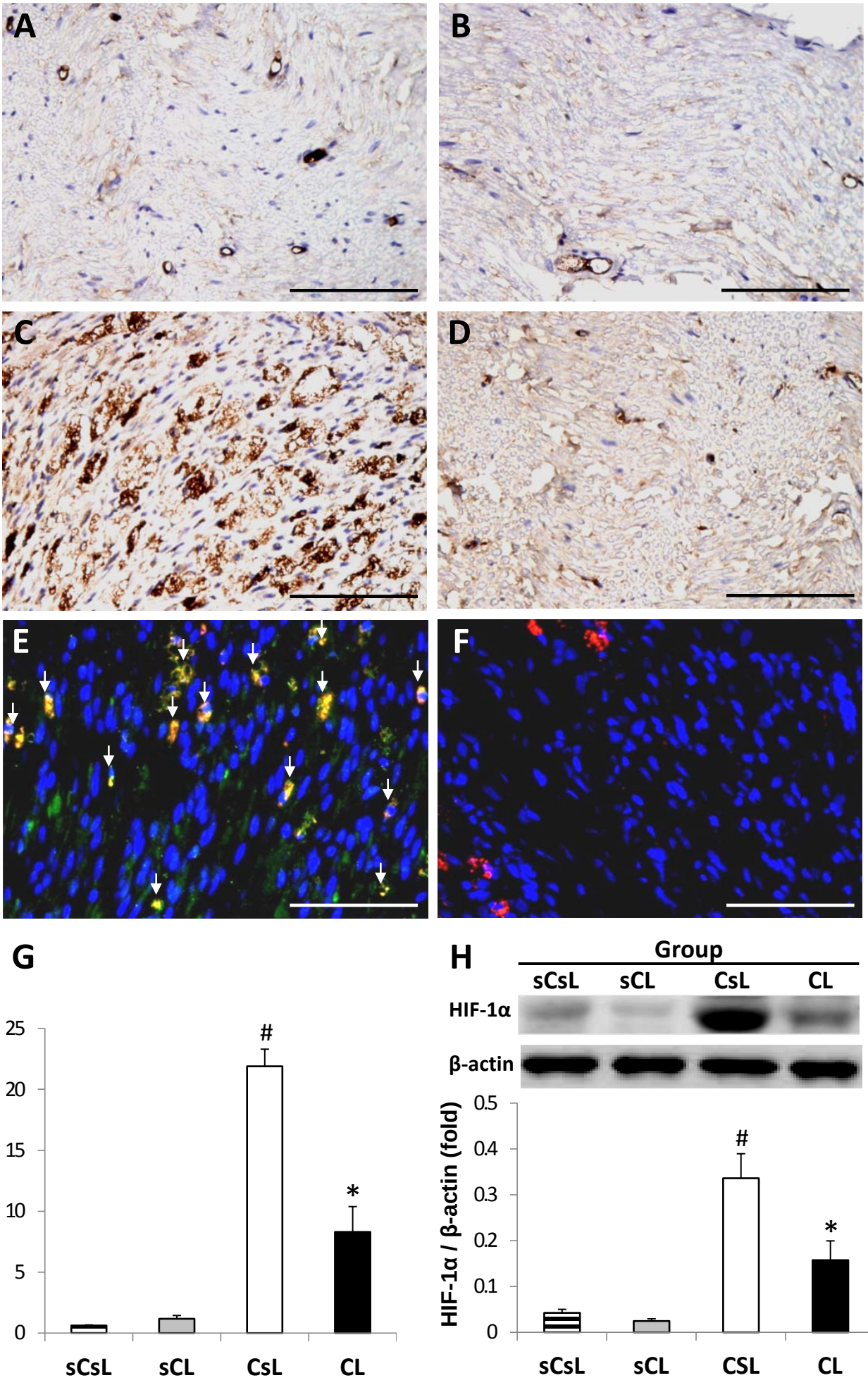
A
B
C
D
E
F
G
HIF-1α-positive stained area (%)
25
20
15
10
5
0
#
*
sCsL
sCL
CsL
CL
H
Group
sCsL
sCL
CsL
CL
HIF-1α
β-actin
HIF-1α / β-actin (fold)
0.5
0.4
0.3
0.2
0.1
0
#
*
sCsL
sCL
CSL
CL

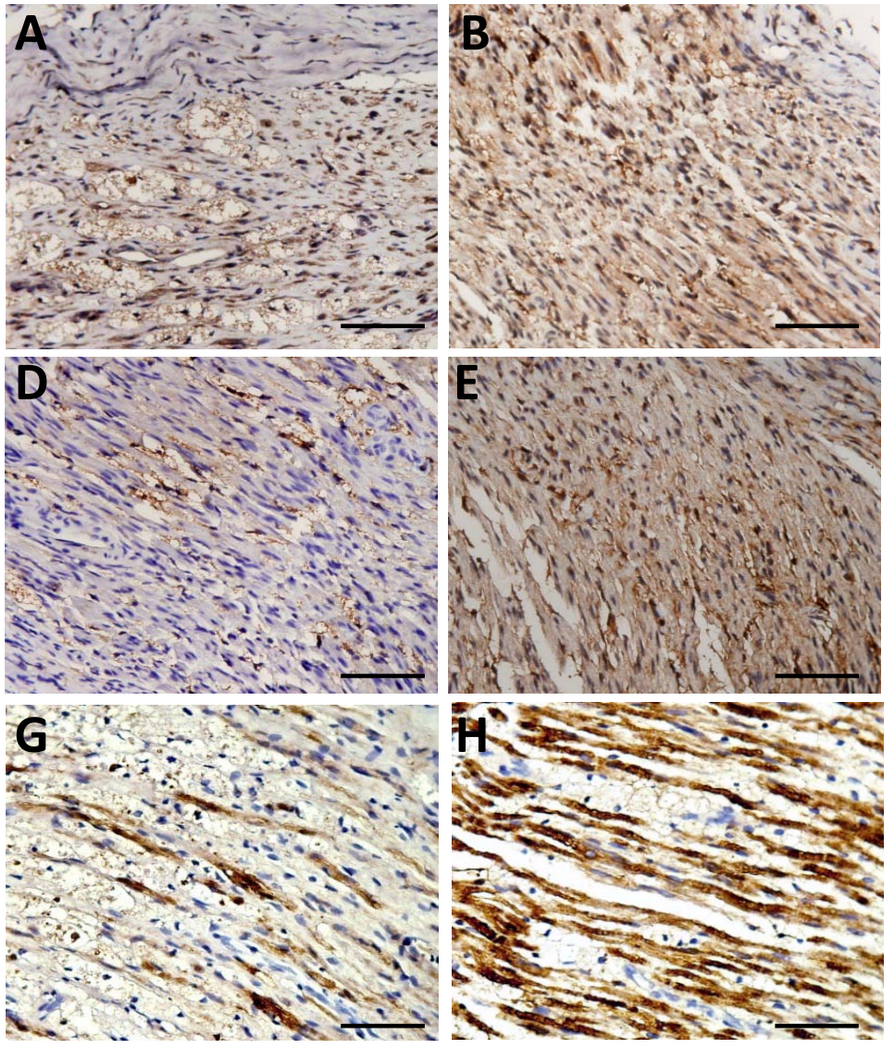
A
B
D
E
G
H

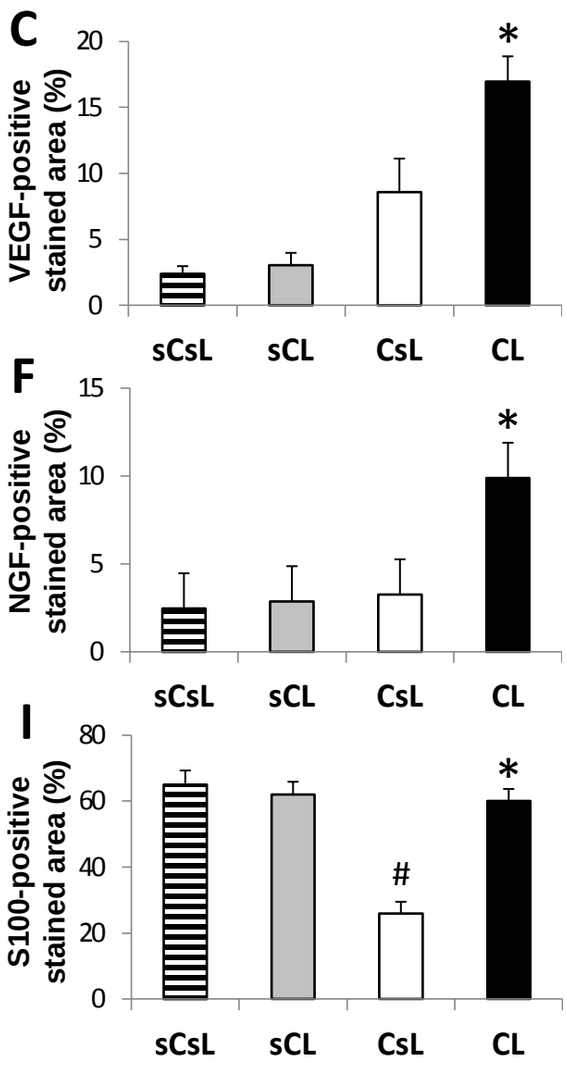
C
VEGF-positive stained area (%)
20
15
10
5
0
*
sCsL
sCL
CsL
CL
F
NGF-positive stained area (%)
15
10
5
0
*
sCsL
sCL
CsL
CL
I
S100-positive stained area (%)
80
60
40
20
0
*
#
sCsL
sCL
CsL
CL

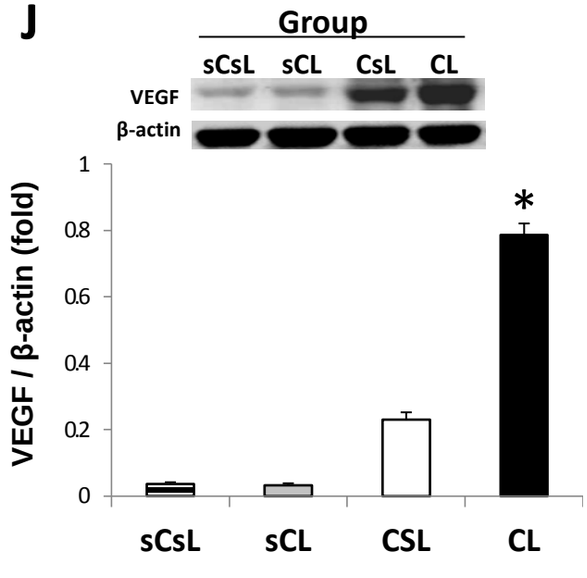
J
Group
sCsL
sCL
CsL
CL
VEGF
β-actin
VEGF / β-actin (fold)
1
0.8
0.6
0.4
0.2
0
*
sCsL
sCL
CSL
CL

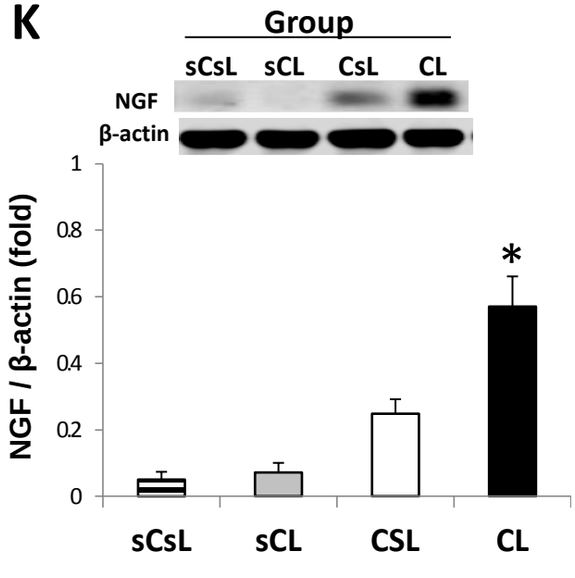
K
Group
sCsL
sCL
CsL
CL
NGF
β-actin
NGF / β-actin (fold)
1
0.8
0.6
0.4
0.2
0
*
sCsL
sCL
CSL
CL